Statistics of wave functions and currents induced by spin-orbit interaction in chaotic billiards

Evgeny N. Bulgakov[1,2] and Almas F. Sadreev[1,2,3]
[1]*Kirensky Institute of Physics, 660036, Krasnoyarsk, Russia*
[2]*Astaf'ev Krasnoyarsk Pedagogical University, 660049, Lebedeva, 89, Russia*
[3]*IFM, Linköping University, S-581 83 Linköping, Sweden*
(Received 31 January 2004; revised manuscript received 3 September 2004; published 18 November 2004)

We show that the wave function and current statistics in chaotic Robnik billiards crucially depend on the constant of the spin-orbit interaction (SOI). For small constant the current statistics is described by universal current distributions derived for slightly opened chaotic billiards [Saichev *et al.*, J. Phys. A. **35**, L87 (2002)] although one of the components of the spinor eigenfunctions is not universal. For strong SOI both components of the spinor eigenstate are complex random Gaussian fields. This observation allows us to derive the distributions of spin-orbit persistent currents which well describe numerical statistics. For intermediate values of the statistics of the eigenstates and currents, both are deeply nonuniversal.

DOI: 10.1103/PhysRevE.70.056211 PACS number(s): 05.45.Mt, 05.60.Gg, 73.23.Ad

I. INTRODUCTION

The physical properties of mesoscopic systems are strongly affected by quantum interference effects, and one of the intriguing phenomena is the persistent current in a ring threaded by a magnetic flux [2,3]. Since electrons have spin as well as charge, it is therefore of interest to study if the spin degree of freedom can play some effective and significant role in persistent current phenomena. Based on the discovery of the geometric phase [4], many authors have investigated the persistent currents in one-dimensional (1D) rings induced by the geometric phases, which originate from the interplay between an electron's orbital and spin degrees of freedom [5–9]. General properties of charge and spin transport in 2D systems with the Rashba [10] spin-orbit coupling have acquired intense attention lately [11,12].

First the persistent current in ballistic chaotic billiards was considered by Kawabata [13]. He derived the semiclassical formula of the typical mean value of the persistent current for a single billiard and the average persistent current for an ensemble of billiards at finite temperature. These formulas are used to show that the persistent current for chaotic billiards is much smaller than that for integrable ones. The persistent currents in the ballistic regime therefore become an experimental tool to search for the quantum signature of classical chaotic and regular dynamics. The nearest neighbor level statistics and nodal point distribution in a rectangular quantum dot with the Rashba spin-orbit interaction (SOI) were considered recently by Berggren and Ouchterlony [14].

In the present article we consider the statistics of the persistent currents produced by SOI in chaotic billiards such as the Robnik (cardioid) one. For open chaotic billiards (without SOI) the current statistics, as was shown [1], has very simple exponential behavior and this was confirmed experimentally for microwave transmission through chaotic billiards [15,16].

In III-V semiconductor heterostructures SOI is intrinsic because of the lack of inversion symmetry. For the two-dimensional electron gas confined in a quantum dot (QD) by a gate voltage the Hamiltonian for an electron in the electric field **E** and magnetic field **B** directed along the z axis is

$$H = \frac{1}{2m^*}\left(\mathbf{p} - \frac{e}{c}\mathbf{A}\right)^2 + \hbar K\left[\sigma \times \left(\mathbf{p} - \frac{e}{c}\mathbf{A}\right)\right]_z, \qquad (1)$$

where $m^* = 0.023m$ is the effective mass and $\hbar^2 K = 6 \times 10^{-10}$ eV cm is the SOI coefficient in an InAs structure [17]. The dominant mechanism for the SOI in a two-dimensional electron gas (2DEG) is attributed to the Rashba term [12,18]. Using the characteristic scale of a QD R, we rewrite Eq. (1) in dimensionless form for $\mathbf{B} = \mathbf{0}$

$$\tilde{H} = \begin{pmatrix} -\nabla^2 & \beta\left(\frac{\partial}{\partial x} - i\frac{\partial}{\partial y}\right) \\ \beta\left(-\frac{\partial}{\partial x} - i\frac{\partial}{\partial y}\right) & -\nabla^2 \end{pmatrix}, \qquad (2)$$

where $\beta = 2m^* KR$. We consider that the electric field is directed normal to the plane of the QD. The confining potential is approximated by a hard wall potential to consider the QD as a billiard. An expression for current density can be obtained as follows [19]:

$$\tilde{j} = \mathbf{j}/\mathbf{j}_0 = -c\frac{\delta\langle H\rangle}{j_0 \delta \mathbf{A}} = \mathrm{Im}(\Psi^\dagger \boldsymbol{\nabla} \Psi) + \beta \Psi^\dagger (\mathbf{n} \times \sigma)\Psi, \quad (3)$$

where $j_0 = e\hbar/m^* L^3$.

Historically, McDonnell and Kauffmann first numerically revealed the complicated eigenfunction structures in a closed two-dimensional Bunimovich billiard [20]. It is well known that the statistics of the eigenfunction's amplitude obeys a Gaussian distribution. The evolution of statistics of the eigenspinor eigenfunctions in a chaotic billiard with growth of the SOI constant was considered in [21]. It was shown that the eigenfunction statistics crucially depend on the ratio between the squared SOI constant and the eigenenergy. If this ratio is small, one of the eigenstate components is a complex random Gaussian field (RGF), whereas the other is not and depends on the billiard boundary. In the opposite case, both spinor components are independent RGFs with the same

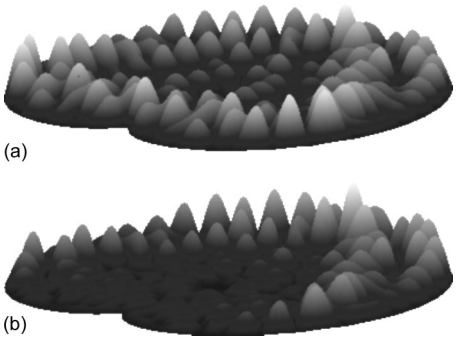

FIG. 1. Spatial structures of (a) the upper $|\phi|$ and (b) the lower $|\chi|$ components of the spinor eigenfunction of a cardioid with parameter $\kappa=0.45$ for $\epsilon=522.251$ and $\beta=0.25$.

variances [21]. Here we consider the statistics of the persistent currents induced by spin-orbit interaction in a chaotic Robnik billiard.

The Schrödinger equation with the Hamiltonian (2) takes the following dimensionless form:

$$-\nabla^2\phi+\beta L\chi=\epsilon\phi,$$

$$-\nabla^2\chi+\beta L^+\phi=\epsilon\chi, \tag{4}$$

where $L=\partial/\partial x-i\partial/\partial y$, $\epsilon=2m^*R^2E/\hbar^2$. We imply the Dirichlet boundary conditions for both components of the eigenstate in the Robnik [22] billiard. Numerically, for solution of Eq. (4) we used the boundary integral method [23] developed with account of SOI. However, for small and large SOI constants Eq. (4) allows analytical estimations.

II. WEAK SPIN-ORBIT INTERACTION

For small SOI constant $\beta\ll\sqrt{\epsilon}$ we can approximate a solution of Eq. (4) as [21]

$$\phi=\psi_b+O(\beta) \tag{5}$$

$$\chi=-\frac{\beta}{2}[(x+iy)-C]\psi_b=-\frac{\beta}{2}[(x-x_0)+i(y-y_0)]\psi_b,$$

where ψ_b are eigenfunctions of the Schrödinger equation $-\nabla^2\psi_b=\epsilon_b\psi_b$ for $\beta=0$, and $C=x_0+iy_0$ is some arbitrary complex constant. The solution (5) demonstrates that the second component $\chi(x,y)$ linearly increases in the billiard region, as it is clearly seen from the numerical solution shown in Fig. 1. Then it follows from Eq. (5) that, if the eigenfunctions ψ_b are a random Gaussian field, the upper component ϕ is also a RGF, whereas the lower component χ is not. Numerically this result was demonstrated in [21] for the cardioid (Robnik) billiard

$$(x^2+y^2-\kappa^2)^2=x^2+y^2+2\kappa x+\kappa^2. \tag{6}$$

For the second Kramers degenerate state the lower component is correspondingly a RGF, whereas the upper component is not.

Using these results we can find the current distributions. Substituting the solution (5) into Eq. (3) one can easily find

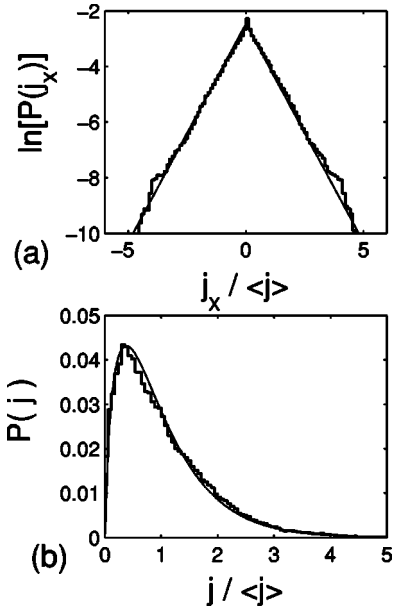

FIG. 2. Current distributions $P(j_x)$ (a) and $P(j)$ (b) for the Robnik billiard for $\epsilon=2013.2, \kappa=0.45, \beta=0.1, \langle j\rangle=2.7\times10^{-6}$. The current distributions (7) and (8) are shown by thin solid lines.

that the current is determined by only one component ϕ with accuracy $O(\beta^2)$. Since this state is a complex RGF it immediately follows that the current distributions are given by formulas derived in [1,15]:

$$P(j_\alpha)=\frac{\pi}{4\langle j\rangle}\exp\left(-\frac{\pi|j_\alpha|}{2\langle j\rangle}\right),\quad \alpha=x,y, \tag{7}$$

$$P(j)=\frac{\pi^2 j}{4\langle j\rangle^2}K_0\left(\frac{\pi j}{2\langle j\rangle}\right), \tag{8}$$

where $j=|\mathbf{j}|$, $K_0(z)$ is the modified Bessel function of the second kind, $\langle j\rangle=(\pi\epsilon/4)(\langle u^2\rangle\langle v^2\rangle-\langle uv\rangle^2)$, and u and v are real and imaginary parts of the eigenfunction of the billiard $\phi=u+iv$.

The numerical results for current statistics compared with analytical distributions (7) and (8) are shown in Fig. 2. The distribution $P(j_y)$ is not shown in Fig. 2 since it is very close to $P(j_x)$. One can see good agreement of the theory with the numerics for small SOI constant.

III. STRONG SPIN-ORBIT INTERACTION

Using the equality $L^+L=-\nabla^2$ we can obtain from Eq. (4)

$$\chi=\frac{\beta L^+}{\epsilon-L^+L}\phi,\quad \phi=\frac{\beta L}{\epsilon-L^+L}\chi. \tag{9}$$

Substituting the first relation into Eq. (4) we obtain

$$[\nabla^4+(\beta^2+2\epsilon)\nabla^2+\epsilon^2]\phi=0. \tag{10}$$

A solution of this equation can be presented as the superposition

$$\phi = a\phi_1 + b\phi_2, \tag{11}$$

where a and b are arbitrary complex coefficients and where each function satisfies to the following equations

$$-\nabla^2\phi_1 = \left(\epsilon + \frac{\beta^2}{2} + \frac{\beta^2}{2}\sqrt{1+\frac{4\epsilon}{\beta^2}}\right)\phi_1, \tag{12}$$

$$-\nabla^2\phi_2 = \left(\epsilon + \frac{\beta^2}{2} - \frac{\beta^2}{2}\sqrt{1+\frac{4\epsilon}{\beta^2}}\right)\phi_2. \tag{13}$$

Although these equations formally look like the Schrödinger ones for the billiard, in fact, they are not because the Dirichlet boundary conditions are implied only on ϕ but not separately on ϕ_1 and ϕ_2.

For strong SOI $\beta^2 \gg \epsilon$ Eqs. (12) and (13) can be written as follows:

$$-\nabla^2\phi_1 \approx (2\epsilon + \beta^2)\phi_1, \tag{14}$$

$$-\nabla^2\phi_2 \approx \frac{\epsilon^2}{\beta^2}\phi_2. \tag{15}$$

Correspondingly, one can see that the characteristic wavelength of the first contribution ϕ_1 is $\lambda_1 \sim 2\pi/\sqrt{2\epsilon+\beta^2} \approx 2\pi/\beta$ while the second contribution ϕ_2 has the characteristic wavelength $\lambda_2 \sim 2\pi\beta/\epsilon$. These characteristic lengths are demonstrated in Fig. 5 below. Moreover for $\beta \gg \epsilon$ we can neglect ϵ in the denominator of Eq. (9) and rewrite Eq. (9) as

$$\chi \approx -\frac{1}{\beta}L^\dagger\phi, \quad \phi \approx -\frac{1}{\beta}L\chi. \tag{16}$$

As in a 2DEG the solution ϕ consists of a fast fluctuating part ϕ_1 and a slowly varying part ϕ_2. Substituting Eq. (11) into the first relation (16) we obtain that the slowly varying part contributes to the lower component χ as $\epsilon/\beta^2 \ll 1$. Because of the second relation (16) the same result takes place for the upper component ϕ. Thus, we can ignore the slowly varying part in the solution in Eq. (11) ($\phi \approx \phi_1$). Then Eq. (14) becomes the Schrödinger equation with spectra $2\epsilon+\beta^2$ and eigenfunctions ϕ where ϕ is approximately a real function. However, because of the Kramers degeneracy the eigenstate is an arbitrary superposition $(A+Bi\hat{C}\sigma_y)\Psi$ with complex A and B where $\hat{C}$ is the operator of complex conjugation. As a result in the numerics as a rule we obtain both components of the spinor eigenstate as complex functions.

IV. CURRENT STATISTICS

As we consider the chaotic billiard, the eigenfunctions are mainly RGFs [20]. Bouncing modes are exceptional. Therefore in the general case the upper component can be presented as $\phi = u + iv$ where u and v are real RGFs. Although u and v might be statistically dependent, there is a phase transformation $\phi \to e^{i\theta}\phi = p + iq$ which makes p and q statistically independent $\langle pq\rangle = 0$ [1]. Then it follows from Eq. (16) that the lower component χ takes the form

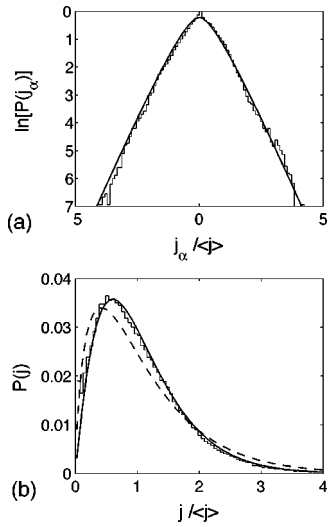

FIG. 3. Current distributions $P(j_x)$ (a) and $P(j)$ (b) for the Robnik billiard for $\kappa = 0.45$, $\epsilon = 57.684$, $\beta = 50$, $\tilde{\beta} = -1.056$, $\alpha = -0.043$, $\langle j\rangle = 3.373$. (a) The numerical current distribution $\ln[P(j_x)]$ (thin solid line) is compared with Eq. (29) (thick solid line). (b) The numerical current distribution $P(j)$ (thin solid line) is compared with formulas (8) (dashed line) and (30) (thick solid line). The statistics was performed over 200 000 points.

$$\chi = t + iw, \quad \beta t = p_x - q_y, \quad \beta w = q_x + p_y. \tag{17}$$

Since the functions p and q are statistically independent RGFs, their derivatives are also statistically independent RGFs. Therefore the functions t and w are statistically independent RGFs. Moreover, if some function f is obeying the Dirichlet boundary condition, then $\langle f\nabla f\rangle = 0$, where

$$\langle\cdots\rangle = \frac{1}{A}\int d^2\mathbf{x}\ldots, \tag{18}$$

and A is the area of the billiard. Hence we can state that all four functions p, q, t, w are statistically independent RGFs. These conclusions are completely confirmed in the numerics [21] for strong SOI.

In view of the above let us present the eigenstate as

$$\Psi = \begin{pmatrix}\phi(\mathbf{r})\\ \chi(\mathbf{r})\end{pmatrix} = \begin{pmatrix}p(\mathbf{r}) + iq(\mathbf{r})\\ t(\mathbf{r}) + iw(\mathbf{r})\end{pmatrix}. \tag{19}$$

Then the probability current (3) can be written as follows:

$$\tilde{\mathbf{j}} = p\,\boldsymbol{\nabla} q - q\,\boldsymbol{\nabla} p + t\,\boldsymbol{\nabla} w - w\,\boldsymbol{\nabla} t + \beta\mathbf{e}_x(pw - qt) - \beta\mathbf{e}_y(pt + qw), \tag{20}$$

where $\mathbf{e}_x$ and $\mathbf{e}_y$ are the unit vectors directed along the x and y axes, respectively. In order to derive the current distributions [say, the distribution $P(j_x)$], we use the characteristic function [1]

$$\Theta(a_x) = \langle e^{ia_x j_x}\rangle. \tag{21}$$

From Eqs. (20) and (21) it follows that we need eight RGFs $\Phi = (p\ t_x\ q\ w_x\ t\ p_x\ w\ q_x)$, $p_x = \partial p/\partial x, \ldots$, with the probability density of these fields given by [24]

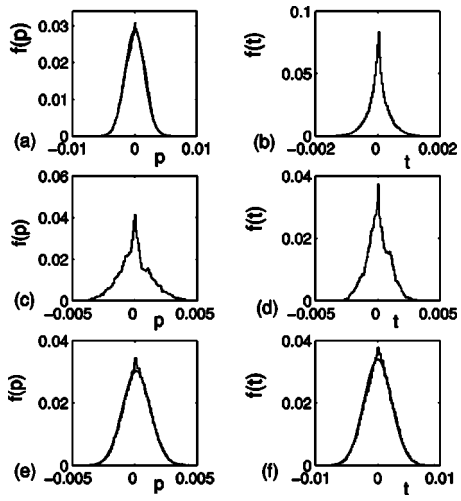

FIG. 4. The numerical distributions of the real parts of the upper (left) and lower components (right) of the eigenspinor state for three characteristic values of β. (a), (b) $\beta^2 \ll \epsilon$ ($\beta=0.25, \epsilon=522.25$), (c), (d) $\beta^2 \sim \epsilon$ ($\beta=10, \epsilon=87.57$), and (e), (f) $\beta^2 \gg \epsilon$ ($\beta=50, \epsilon=57.684$). Solid lines show the Gaussian distributions.

$$f(\Phi) = \frac{1}{4\pi^2\sqrt{\det K}} \exp\left(-\frac{1}{2}\Phi^+ K^{-1}\Phi\right) \tag{22}$$

where the covariant matrix consists of mean values $K = \langle \Phi^+ \Phi \rangle$. In numerical computations we use that the average over the billiard area (18) is equivalent to an average over an eight-dimensional GRF Φ:

$$\langle \cdots \rangle = \int d^8\Phi \; f(\Phi) \ldots . \tag{23}$$

Equation (17) establishes that there are only the following correlations: $\langle tp_x \rangle = -\langle pt_x \rangle = (1/\beta)\langle p_x^2 \rangle$ and $\langle wq_x \rangle = -\langle qw_x \rangle = (1/\beta)\langle q_x^2 \rangle$. Therefore the covariant 8×8 matrix is decomposed into four 2×2 matrices: $K = \oplus_{j=1}^4 K_j$ with

$$K_1 = \begin{pmatrix} \langle p^2 \rangle & \langle pt_x \rangle \\ \langle pt_x \rangle & \langle t_x^2 \rangle \end{pmatrix}, \quad K_2 = \begin{pmatrix} \langle q^2 \rangle & \langle qw_x \rangle \\ \langle qw_x \rangle & \langle w_x^2 \rangle \end{pmatrix},$$

$$K_3 = \begin{pmatrix} \langle t^2 \rangle & \langle tp_x \rangle \\ \langle tp_x \rangle & \langle p_x^2 \rangle \end{pmatrix}, \quad K_4 = \begin{pmatrix} \langle w^2 \rangle & \langle wq_x \rangle \\ \langle wq_x \rangle & \langle q_x^2 \rangle \end{pmatrix}. \tag{24}$$

Let us estimate the matrix elements of the covariant matrix. Because of normalization of the eigenstate $\int d^2\mathbf{x}\; \Psi^\dagger \Psi = 1$ and Eq. (18) we obtain $\langle p^2 \rangle \sim 1/A$. The area of the cardioid billiard $A = \pi(1+2\kappa^2) \approx 4.414$ for $\kappa = 0.45$. Moreover, from Eq. (17) we obtain $\langle tp_x \rangle = \beta \langle t^2 \rangle \sim \beta/A$, $\langle p_x^2 \rangle \approx \frac{1}{2}\langle (\nabla p)^2 \rangle \approx \beta^2 \langle p^2 \rangle$.

Numerical calculations give for $\beta = 50$ the following result ($\epsilon = 57.684$):

$$AK_1 = \begin{pmatrix} 0.247 & 6.46 \\ 6.46 & 340.9 \end{pmatrix}, \quad AK_2 = \begin{pmatrix} 0.26 & 6.6 \\ 6.6 & 319.2 \end{pmatrix},$$

$$AK_3 = \begin{pmatrix} 0.246 & -6.46 \\ -6.46 & 305.7 \end{pmatrix}, \quad AK_4 = \begin{pmatrix} 0.247 & -6.6 \\ -6.6 & 319.2 \end{pmatrix}. \tag{25}$$

One can see that these numerical results agree well with the above estimations for correlations. The eight-dimensional probability function is decomposed as

$$f(\Phi) = f(u,t_x) f(v,w_x) f(t,u_x) f(w,v_x), \tag{26}$$

where

$$f(a,b) = \frac{1}{2\pi} \exp\left(-\frac{1}{2\Gamma}(\langle b^2 \rangle a^2 + \langle a^2 \rangle b^2 - 2\langle ab \rangle ab)\right), \tag{27}$$

$\Gamma = \langle a^2 \rangle \langle b^2 \rangle - \langle ab \rangle^2$. As Eq. (25) shows, we can take approximately equal Γ for each pair of RGFs in the distribution function (26) for strong SOI constant β. Then a simple but tedious procedure of integration over eight GRFs gives us the following form for the characteristic function (21):

$$\Theta(a_x) \approx \frac{1}{(1+\Gamma a_x^2)^2 + 4\tilde{\beta}^2 \langle p^2 \rangle^2 a_x^2}, \tag{28}$$

where $\Gamma = \langle p^2 \rangle \langle t_x^2 \rangle - \langle pt_x \rangle^2 \approx \langle q^2 \rangle \langle w_x^2 \rangle - \langle qw_x \rangle^2 \approx \langle t^2 \rangle \langle p_x^2 \rangle - \langle tp_x \rangle^2 \approx \langle w^2 \rangle \langle q_x^2 \rangle - \langle wq_x \rangle^2$, $\tilde{\beta} = \beta/2 - \langle pt_x \rangle / \langle p^2 \rangle$. Following [1] we have for the distribution $P(j_x)$

$$P(j_x) = \frac{1}{2\pi} \int_{-\infty}^{\infty} \Theta(|a_x|) \exp(-ia_x j_x) da_x$$

$$= \frac{1}{8\alpha\sqrt{1+\alpha^2}\sqrt{\Gamma}} \left[\frac{1}{a_1} \exp\left(-\frac{a_1 |j_x|}{\sqrt{\Gamma}}\right) - \frac{1}{a_2} \exp\left(-\frac{a_2 |j_x|}{\sqrt{\Gamma}}\right) \right] \tag{29}$$

where $a_{1,2} = \sqrt{1+\alpha^2} \mp \alpha$, $\alpha = \tilde{\beta}\langle p^2 \rangle / \sqrt{\Gamma}$.

The same expression can be obtained for $P(j_y)$. In order to derive the distribution function for j let us consider the joint distribution function. Following [1] we obtain

$$P(j) = j \int_0^\infty a \, da \, J_0(aj) \Theta(a). \tag{30}$$

The numerical current distributions are shown in Fig. 3, compared with the analytical distributions (29), (8), and (30) with $\langle j \rangle$ calculated numerically from Eq. (30). The comparison demonstrates very good coincidence of theory with numerics. The numerical distribution $P(j_y)$ is not shown in Fig. 3(a) since it is very close to $P(j_x)$. To ensure that the numerical computation of the spinor eigenfunctions in the Robnik billiard was accurate for the large SOI constant $\beta = 50$ we chose the eigenenergy rather low, $\epsilon = 57.684$. It gives the characteristic wavelength of the eigenfunction $\lambda = 2\pi/\beta \approx 0.1$.

V. CONCLUSION

Finally we demonstrate the statistics of the real parts of the eigenfunctions for three characteristic values of the SOI

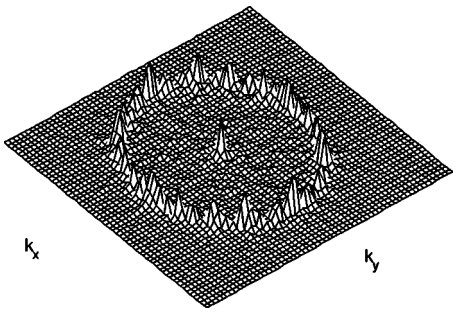

FIG. 5. The Fourier image of the real part of the upper component p for $\beta^2 \gg \epsilon$ ($\beta=50$, $\epsilon=57.684$).

constant (Fig. 4). The statistics of the imaginary parts has the same behavior. One can see that for small SOI only the upper component is a complex RGF while the statistics of the lower component depends on the billiard geometry [21]. For moderate constants of SOI ($\beta^2 \sim \epsilon$) [Figs. 4(c) and 4(d)] the wave function statistics as well as the current statistics are deeply nonuniversal. Finally, for the strong SOI constant ($\beta^2 \gg \epsilon$), both components of the eigenspinor are complex RGFs as is seen from Figs. 4(e) and 4(f). However, as shown in Figs. 4(e) and 4(f) we can see small deviations from the Gaussian distributions near $p=0$ and $t=0$ which are related to the small second contribution in Eq. (11). This contribution can be resolved if we plot the Fourier transform of some component of the eigenspinor, say, p as shown in Fig. 5. Mainly the Fourier components are collected in a circle with $|k|=\sqrt{\beta^2+2\epsilon}$ in accordance with Eq. (14). There are also a few Fourier components near $|k|=0$ which are contributed by the solution ϕ_2 of Eq. (15). However, Fig. 5 demonstrates that the second contribution ϕ_2 with characteristic $k_2 \approx \epsilon/\beta$ is negligibly small in comparison to the first contribution ϕ_1 with characteristic $k_1 \approx \beta$.

It is promising that experimental techniques to image wave functions and coherent electron flows in semiconductor devices are becoming available using scanned probe microscopes [25]. However, these techniques hardly allow us to measure current statistics. Microwave billiards are remarkable equivalents of quantum mechanics [26]. As a result, Stöckmann and co-workers measured current and vortex statistics in chaotic microwave billiards [15,16]. Therefore the most promising way to measure spin-orbit currents is to find the equivalent of the Rashba Hamiltonian (2) in electromagnetic systems. Recently we have found such a correspondence of the Rashba SOI in an infinitely long microwave waveguide filled with ferrite [27] with a cross section equal to that of the billiard. The longitudinal component of the electric field corresponds to the component ϕ, while the longitudinal component of the magnetic field relates to the derivative of χ. Although the boundary conditions in this system are different from the Dirichlet boundary conditions implied on the quantum billiard, we believe that the type of boundary conditions is not important for statistics of eigenfunctions because locally the eigenfunction can be presented as a random superposition of plane waves (the Berry function [28]). The role of the boundaries in the statistical properties of the eigenfunctions of the chaotic billiard was studied recently in [29,30]. It was shown that the boundaries are responsible for logarithmic corrections in the long-range correlation properties of the eigenfunctions and for depletion of nodal points near the boundary.

ACKNOWLEDGMENTS

A.S. is grateful to K.-F. Berggren for numerous fruitful discussions. This work was supported by the Russian Foundation for Basic Research (RFBR Grant No. 03-02-17039). A.S. acknowledges the support of the Swedish Royal Academy of Sciences.

[1] A. I. Saichev, H. Ishio, A. F. Sadreev, and K.-F. Berggren, J. Phys. A **35**, L87 (2002).
[2] M. Büttiker, Y. Imry, and R. Landauer, Phys. Lett. **96A**, 365 (1983); R. Landauer and M. Büttiker, *ibid.* **54**, 2049 (1985).
[3] Y. Gefen, Y. Imry, and M. Ya. Azbel, Phys. Rev. Lett. **52**, 129 (1984).
[4] M. V. Berry, Proc. R. Soc. London, Ser. A **392**, 45 (1984).
[5] Y. Meir, Y. Gefen, and O. Entin-Wohlman, Phys. Rev. Lett. **63**, 798 (1989).
[6] H. Mathur and A. D. Stone, Phys. Rev. Lett. **68**, 2964 (1992).
[7] A. V. Balatsky and B. L. Altshuler, Phys. Rev. Lett. **70**, 1678 (1993).
[8] S. Oh and C. M. Ryu, Phys. Rev. B **51**, 13 441 (1995).
[9] A. V. Chaplik and L. I. Magarill, Superlattices Microstruct. **18**, 321 (1995).
[10] Yu. A. Bychkov and E. I. Rashba, JETP Lett. **39**, 78 (1984).
[11] E. G. Mishchenko and B. I. Halperin, Phys. Rev. B **68**, 045317 (2003).
[12] E. I. Rashba, Phys. Rev. B **68**, 241315(R) (2003).
[13] S. Kawabata, Phys. Rev. B **59**, 12 256 (1999).
[14] K.-F. Berggren and T. Ouchterlony, Found. Phys. **31**, 233 (2001).
[15] M. Barth and H.-J. Stöckmann, Phys. Rev. E **65**, 066208 (2002).
[16] Y.-H. Kim, M. Barth, and H.-J. Stöckmann, Phys. Rev. B **65**, 165317 (2002).
[17] A. G. Aronov and Y. B. Lyanda-Geller, Phys. Rev. Lett. **70**, 343 (1993).
[18] J. Nitta, T. Akazaki, H. Takayanagi, and T. Enoki, Phys. Rev. Lett. **78**, 1335 (1997).
[19] L. D. Landau and E. M. Lifshitz, *Quantum Mechanics: Non-Relativistic Theory* (Pergamon, New York, 1977), chap. XVII.
[20] S. W. McDonald and A. N. Kaufman, Phys. Rev. Lett. **42**, 1189 (1979); Phys. Rev. A **37**, 3067 (1988).
[21] E. N. Bulgakov and A. F. Sadreev, JETP Lett. **78**, 443 (2003).
[22] M. Robnik, J. Phys. A **16**, 3971 (1983).
[23] R. J. Riddel, Jr., J. Comput. Phys. **31**, 21 (1979); **31**, 42 (1979).

[24] K. J. Ebeling, *Statistical Properties of Random Wave Fields in Physical Acoustics: Principles and Methods* (Academic, New York, 1984).
[25] M. A. Topinka *et al.*, Nature (London) **410**, 183 (2001).
[26] H.-J. Stöckmann, *Quantum Chaos: An Introduction* (Cambridge University Press, Cambridge, U.K., 1999).
[27] E. N. Bulgakov and A. F. Sadreev, cond-mat/0404072.
[28] M. V. Berry, J. Phys. A **10**, 2083 (1977).
[29] M. V. Berry, J. Phys. A **35**, 3025 (2002).
[30] M. V. Berry and H. Ishio, J. Phys. A **35**, 5961 (2002).